

PREPRINT

Author-formatted, not peer-reviewed document posted on 26/05/2026

DOI: <https://doi.org/10.3897/arphapreprints.e201191>

**Skeleton growth pattern of a late Cambrian - early
Ordovician radiolarian species revealed by X-ray
tomography; Paleobiological implications**

Taniel Danelian, Lusine Harutyunyan, Rémi Habert,  Laurenz Schröer,  Veerle Cnudde

1 **Skeleton growth pattern of a late Cambrian - early Ordovician radiolarian species revealed by X-**
2 **ray tomography; Paleobiological implications.**

3
4 Lusine Harutyunyan^{1,2,3}, Rémi Habert³, Laurenz Schröer⁴, Veerle Cnudde^{4,5}, Taniel Danelian³

5
6 ¹Yerevan State Univ., 1 Alek Manukyan st., Yerevan 0025, Armenia

7 ²Institute of Geological Sciences, NAS RA, 24A, Marshal Baghramyan Avenue, Yerevan 0019, Armenia

8 ³Univ. Lille, CNRS, UMR 8198, Evo-Eco-Paleo, F-59000 Lille, France

9 ⁴PProGRess-UGCT, Department of Geology, Ghent University, 9000 Ghent, Belgium

10 ⁵Environmental hydrogeology, Dept. Earth Sciences, Utrecht Univ., 3584 CB Utrecht, The Netherlands

11 *Corresponding author:* Taniel Danelian (taniel.danelian@univ-lille.fr)

12 **Abstract**

13

14 Micro-computed tomography is increasingly important for the taxonomic analysis of early Palaeozoic
15 radiolarians as it provides the opportunity to conduct detailed observations of the most internal parts of
16 radiolarian skeletons in a non-destructive way. Our observations on 3D models of the species
17 *Protoentactinia gracilispinosa* from lower Tremadocian strata of Newfoundland (Canada) indicate that
18 during the first two stages of growth the skeleton develops symmetrically with respect to the median
19 bar. However, subsequently, progressive reduction of the number of rays placed proximally, combined
20 with full growth of rays distally, results in the formation of an external subglobular shape during stages
21 6 to 8. Although our results confirm the previously assumed growth pattern of the skeleton, they reveal
22 for the first time the number and pattern of branched spicule iterations. More importantly, we establish
23 that some of the stages of skeleton growth are in a preferential direction, highlighting a clear
24 heteropolarity to skeleton development, although the end product is a subspherical spicular test.

25

26 **Key-words**

27 Polycystine radiolaria, Entactinaria, skeletogenesis, micro-computed tomography

28 **Introduction**

29

30 Polycystine radiolaria constitute a diverse group of marine planktic Rhizaria that secrete an aesthetically
31 pleasing skeleton made of amorphous silica. Molecular studies suggest the presence of skeletonless
32 radiolaria since the Late Neoproterozoic (Sandin et al. 2025); however, the presence of polycystine
33 radiolaria in the fossil record has only been confirmed since the early Cambrian (Obut and Iwata 2000;
34 Pouille et al. 2011; Sennikov et al. 2017).

35

36 The Cambrian and Ordovician periods are of key significance for the early evolutionary history of
37 marine organisms, including heterotrophic plankton clades such as polycystine radiolarians. Indeed, the
38 siliceous skeletons of early Palaeozoic radiolarians testify to their significant diversifications and
39 evolutionary changes (Danelian and Monnet 2021, 2026).

40

41 During the last thirty-five years, significant progress has been achieved in the taxonomy and
42 biostratigraphy of early Paleozoic radiolarians (Aitchison et al. 2017; Caridroit et al. 2017; Danelian et
43 al. 2017; Noble et al. 2017). Success relied on the discovery of well-preserved fauna (i.e. Won and
44 Below 1999), which have been carefully described and detailed with 2D imaging techniques, such as
45 scanning electron microscopy (SEM). However, the recent application of micro-computed tomography
46 (micro-CT) on radiolarians (Kachovich et al. 2019) allows the capture of the full 3D complexity of their
47 skeleton development, especially of its most internal parts. The latter are of higher taxonomic
48 significance and thus open new avenues for improved understanding of their internal architectures
49 (Kachovich and Aitchison 2020, 2021; Sheng et al. 2020, 2026a, b).

50

51 Based on Tremadocian (Lower Ordovician) material from Nevada, the species *Protoentactinia*
52 *gracilispinosa* was first introduced by Kozur et al. (1996, p. 253), as the type species of the newly
53 defined genus *Protoentactinia* Kozur et al. (1996), type-genus of the newly defined family

54 Protoentactiniidae. *P. gracilispinosa* was described as a radiolarian bearing a spicular system that was
55 initiated from “a bar-centered entactinarian spicule with 3 terminal rays” at each end; the subglobular
56 skeleton was described as being formed of a repeatedly branching pattern of spicules, which
57 accommodated a nearly spherical inner empty space. The species was later reported from upper
58 Cambrian and lowermost Ordovician strata from western Newfoundland (Won and Iams 2002; Won et al.
59 2005; Pouille et al. 2014). Here, thanks to micro-CT, we provide for the first time details of the different
60 stages of spicular branch re-iterations, the number of spicular rays formed as branches and the overall
61 skeleton growth pattern and dynamics.

62 **Material and methods**

63

64 The single specimen studied here (Fig. 1) comes from a lower Tremadocian radiolarian assemblage,
65 extracted after hydrochloric acid leaching from a limestone sample of the Green Point section (level 23)
66 of the Cow Head Group of Newfoundland (Canada; Pouille et al. 2014). *Protoentactinia gracilispinosa*
67 is abundant in this assemblage (ca. 15% of over 2,000 identified specimens) and has been well
68 documented, with many different specimens, by Pouille et al. (2014). The reader is referred to this paper
69 for further taxonomic and biostratigraphic details.

70

71 Skeleton analysis of the radiolarian specimen was conducted at Ghent University’s Centre of X-ray
72 Tomography (UGCT) in Belgium, thanks to the EXCITE network. These scans were performed using
73 the custom-built Nanowood micro-CT scanner at 70 kV, 4W, and a voxel size of 900 nm. 2322
74 projections were acquired at an exposure time of 1000 ms/projection, resulting in a total scan time of
75 around 40 min. The projections were reconstructed using Octopus Reconstruction (XRE), following the
76 in-house protocol, during which ring filtering and beam hardening corrections were applied. In this
77 study stacks of 2D images were processed using the 3D Slicer software. This open-source software is
78 commonly used to extract structural models from images primarily used for clinical and biomedical
79 applications. Image segmentation delineates regions within an image, in this case structures of the
80 siliceous skeleton. It is essential for visualizing certain structures or for quantifying them (measuring

81 volume, surface area, and shape properties). The segmentation was performed semi-automatically. By
82 manually scanning all the slices (hundreds of 2D images) in three dimensions (X, Y, and Z), and using
83 the segmentation tools provided by the 3D Slicer software, we were able to delineate the areas of
84 interest in the radiolarian specimen by selecting the corresponding grey levels. Each part or segment
85 could then be coloured, facilitating the overall interpretation of each branch within the 3D volume.

86 **Results**

87

88 Colouring dissection allowed us to recognize seven different types of branches (Fig. 2). The most
89 common branch is the trifurcating one, representing the vast majority, but some new rare branches may
90 be single-rayed, or bifurcating, quadrifurcating, pentafurcating and hexafurcating; one single case of
91 heptafurcating branch was also observed. Eight successive stages of skeleton growth are identified.
92 Table 1 lists the number and types of new branches developed at each growth stage and the total
93 number of rays generated at the end of each stage. The first stage represents the initial spicule being
94 formed by two trifurcating branches developed at each opposite side of the median bar (Fig. 3). It is
95 noteworthy that during the first two stages of skeleton growth the branches are exclusively trifurcated.
96 Both the total number of new branches and of new rays increases very rapidly up to stage 5, after which
97 they decrease. It is also worth noting that after stage 2, only a fraction of rays develops new branches;
98 for example, only 17 out of the 18 new rays that are developed at stage 2 produce new branches at stage
99 3. At the end of stage 3, fifty new rays are formed, but only 35 of them branch during stage 4. More
100 remarkably, only a third of the rays that are newly formed during stage 4 will branch during stage 5.
101 Therefore, one may argue that the decreasing trend of spicule development starts during stage 5,
102 although this growth stage results in the largest number of rays produced ever for this specimen.

103

104 In terms of spatial development, nearly half of the final sphere is formed at the end of stage 3. Starting
105 with stage 4, shell growth is clearly oriented distally, away from the initial spicule. However, there is
106 also a trend to form a more complete spherical test. The distally oriented development of the shell is
107 more obvious during stage 5. Most of the branches developed during stage 6 are generated on the

108 opposite side of the initial spicule and in such a way as to form a spherical shell. The few spicules
109 generated during stages 7 and 8 are also developed in such a way as to increase the spherical aspect of
110 the test.

111 **Discussion**

112

113 Based on Tremadocian (Lower Ordovician) material from Nevada, the genus *Protoentactinia* was first
114 introduced by Kozur et al. (1996), as a spicular test initiated by a median bar that bears three rays at
115 each end; the external subglobular test was described as being formed by a repeatedly branching pattern
116 of spicules, which accommodated a nearly spherical inner empty space. Our observations confirm the
117 assessment of Kozur et al. (1996) and further describe the number of iterative branch stages, the number
118 of new spicules formed at each successive stage, as well as the pattern of their distribution spacially.

119

120 The heteropolar development of a polycystine radiolarian skeleton has been recognized until now only
121 for the radiolarians of the order Nassellaria. Here we document for the first time the heteropolar growth
122 of the test in a primitive Entactinarian species. Indeed, the skeleton growth of *Protoentactinia*
123 *gracilispinosa* resembles to some extent the heteropolar development described in Nassellaria, but
124 without the axial symmetry characteristic of Nassellarians. Few are still the studies that provide some
125 insights to the function of the polycystine radiolarians skeleton morphology (i.e. Matsuoka 2007). We
126 may realistically consider that their siliceous skeleton served as an anchoring structure for a better
127 function of the axoflagellates and cytoplasmic extensions. We may also speculate that *P. gracilispinosa*
128 had a cell structure similar to the periaxoplastid-type, as described by Hollande and Enjumet (1960)
129 from cellular observations of living radiolarians from the Western Mediterranean. If such was indeed
130 the case, we may imagine that the axoplast *P. gracilispinosa* was likely positioned close to the initial
131 spicule and that axoflagellates were all oriented antapically away of the axoplast. Such an axoflagellate
132 organisation would be consistent with the directional skeleton growth of *P. gracilispinosa* in spite of its
133 final subsphaerical form.

134

135 **Conclusions**

136

137 Our analysis confirms the initial description provided by Kozur et al. (1996) for *Protoentactinia*
138 *gracilispinosa*; indeed, the subglobular “spongy” test of this entactinarian species is formed by repeated
139 branches of rays starting from two trifurcating branches formed in a crown-shaped arrangement from
140 each termination of an initial spicule composed of a median bar (MB). The skeleton is formed through 8
141 stages of reiterated branches, but the subglobular form mainly develops during stages 3, 4 and 5. The
142 maximum number of branches is manifested in stage 5, with a total of 109 rays, after which their
143 number gradually decreases. Heteropolarity is expressed by the excentric position of the initial spicule,
144 as described by Kozur et al. (1996). However, directional skeleton growth (alike in Nassellarians) is
145 established here for the first time thanks to micro-CT analysis.

146

147 **Acknowledgements**

148

149 This project has received funding from the European Union’s Horizon Europe research and innovation
150 programme under grant agreement no. 101005611 (EXCITE) / 101131765 101131765 (EXCITE²) for
151 Transnational Access conducted at the Centre of X-ray Tomography (UGCT), Ghent University, which
152 is funded by the BOF Special Research Fund (BOF.COR.2022.008). Furthermore, the authors would
153 like to acknowledge the financial support for the Nanowood CT system (BOF Starting Grant,
154 BOFSTG2018000701) as well as the FWO (G00972ON and G019521N) and the Faculty of Bioscience
155 Engineering (FBW-CWO-UGent grant). Views and opinions expressed are, however, those of the
156 authors only and do not necessarily reflect those of the European Union or the European Commission.
157 Neither the European Union nor the granting authority can be held responsible for them. L.
158 Harutyunyan is grateful to the Erasmus + KA171 Program for funding her mobility for studies to the
159 University of Lille the second semester of the year 2024/25. Charlotte Hunt is gratefully acknowledged
160 for editing the English.

161

162

163 **References**

164

- 165 Aitchison JC, Suzuki N, Caridroit M, Danelian T, Noble P (2017) Paleozoic radiolarian biostratigraphy. *Geodiversitas* 39:
166 503–531, <https://doi.org/10.5252/g2017n3a5>.
- 167 Caridroit M, Danelian T, O’Dogherty L, Cuvelier, J, Aitchison JC, Pouille L, Noble P, Dumitrica P, Suzuki N, Kuwahara K,
168 Maletz J, Feng Q (2017) An illustrated catalogue and revised classification of Paleozoic radiolarian genera.
169 *Geodiversitas* 39: 363–417, <https://doi.org/10.5252/g2017n3a3>.
- 170 Danelian T, Aitchison JC, Noble P, Caridroit M, Suzuki N, O’Dogherty L (2017) Historical insights on nearly 130 years of
171 research on Paleozoic radiolarians. *Geodiversitas* 39: 351–361, <https://doi.org/10.5252/g2017n3a2>.
- 172 Danelian T, Monnet C (2021) Early Paleozoic radiolarian plankton diversity and the Great Ordovician Biodiversification
173 Event. *Earth-Science Reviews* 218: 103672, <https://doi.org/10.1016/j.earscirev.2021.103672>.
- 174 Danelian T, Monnet C (2026) Early Paleozoic radiolarian macroevolutionary dynamics and possible relation to global change,
175 *Earth and Environmental Science Transactions of the Royal Society of Edinburgh* 116: 136-145,
176 doi:10.1017/S1755691025100947.
- 177 Hollande A, Enjument M (1960) Cytology, evolution and systematics of Sphaeroidea (Radiolaria). *Archives du Muséum*
178 *national d’histoire naturelle, Paris*, 7: 1-134 (in French).
- 179 Kachovich S, Aitchison JC (2020) Micro-CT study of Middle Ordovician Spumellaria (radiolarians) from western
180 Newfoundland, Canada. *Journal of Paleontology* 94: 417-435, <https://doi.org/10.1017/jpa.2019.88>.
- 181 Kachovich S, Aitchison J C (2021) Middle Ordovician (middle Darriwilian) Archaeospicularia and Entactinaria
182 (radiolarians) from the Table Cove Formation, Piccadilly Quarry, western Newfoundland, Canada. *Journal of*
183 *Paleontology* 95: 913-943, <https://doi.org/10.1017/jpa.2021.18>.
- 184 Kachovich S, Sheng J, Aitchison JC (2019) Adding a new dimension to investigations of early radiolarian evolution.
185 *Scientific Reports* 9(1): 5331, <https://doi.org/10.1038/s41598-019-42771-0>.
- 186 Kozur H, Mostler H, Repetski JE (1996) Well-preserved Tremadocian Radiolaria from the Windfall Formation of the
187 Antelope Range, Eureka County, Nevada, U.S.A. *Geologisch-Paläontologische Mitteilungen Innsbruck* 121: 245-
188 271.
- 189 Matsuoka A (2007) Living radiolarian feeding mechanisms: new light on past marine ecosystems. *Swiss Journal of*
190 *Geosciences* 100 : 273–279 DOI 10.1007/s00015-007-1228-y
- 191 Noble PJ, Aitchison JC, Danelian T, Dumitrica P, Maletz J, Suzuki N, Cuvelier J, Caridroit M, O’Dogherty L (2017)
192 Taxonomy of Paleozoic radiolarian genera. *Geodiversitas* 39: 419–502, <https://doi.org/10.5252/g2017n3a4>.
- 193 Obut OT, Iwata K (2000) Lower Cambrian Radiolaria from the Gorny Altai (southern West Siberia). *Novosti Paleontologii i*
194 *Stratigrafii* 2-3: 33-37.
- 195 Pouille L, Danelian T, Maletz J (2014) Radiolarian diversity changes during the Late Cambrian–Early Ordovician transition
196 as recorded in the Cow Head Group of Newfoundland (Canada). *Marine Micropaleontology* 110: 25-41, 2014.

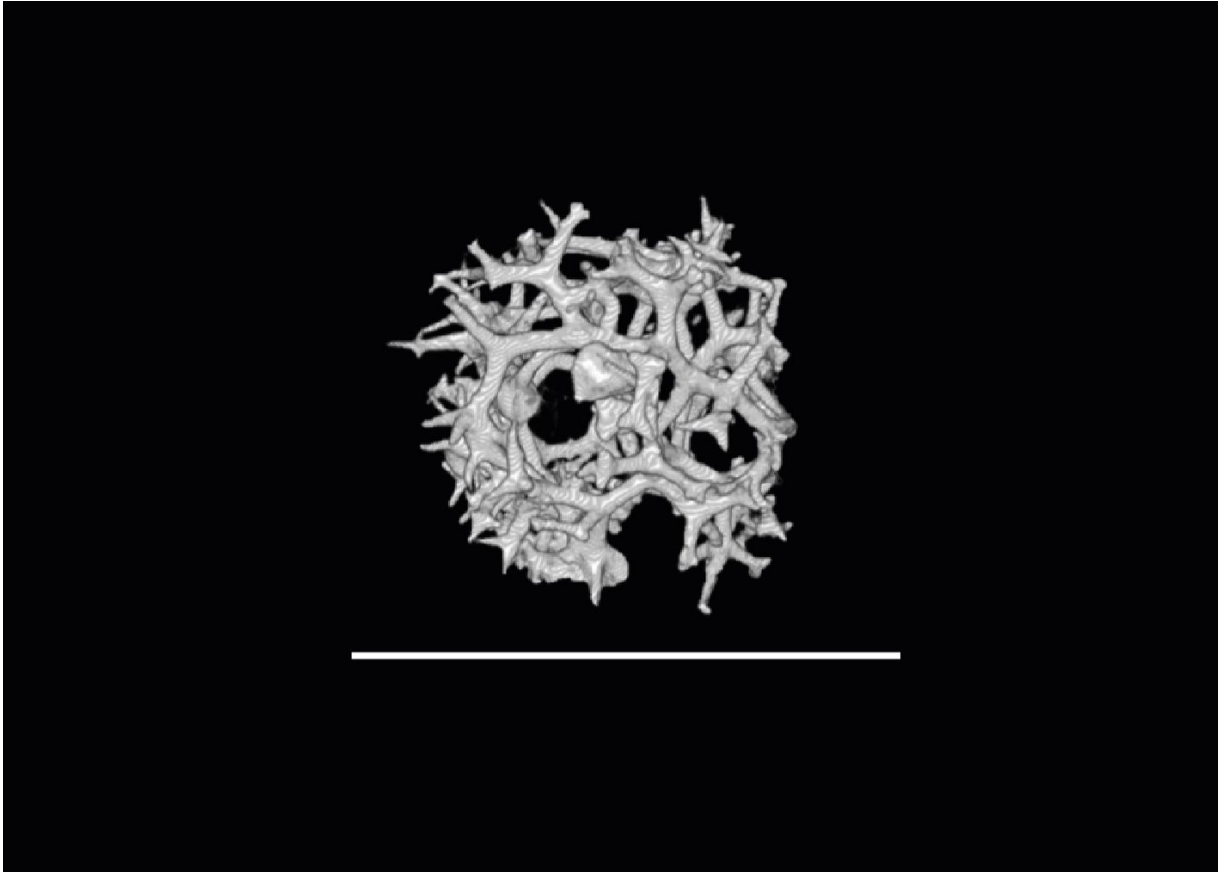
- 197 Pouille L, Obut O, Danelian T, Sennikov N (2011) Lower Cambrian (Botomian) polycystine Radiolaria from the Altai
198 Mountains (southern Siberia, Russia). *Comptes Rendus Palevol* 10 : 627-633.
- 199 Sandin MM, Renaudie J, Suzuki N, Not F (2025) Extant diversity, biogeography, and evolutionary history of Radiolaria.
200 *Current Biology* 35: 2524-2538.
- 201 Sennikov NV, Korovnikov IV, Obut OT, Tokarev DA, Novozhilova NV, Danelian T (2017) The Lower Cambrian of the
202 Salairand Gorny Altai (Siberia) revisited. *Bulletin de la Société Géologique de France* 188(1-2): 1-10. doi:
203 10.1051/bsgf/2017002
- 204 Sheng J, Kachovich S, Aitchison JC (2020) Skeletal architecture of middle Cambrian spicular radiolarians revealed using
205 micro-CT. *Journal of Micropalaeontology* 39: 61-76.
- 206 Sheng J, Aitchison JC, Arhatari BD, Stevenson AW, Kachovich S (2026) Phylogenetic affinity between *Archeoentactinia*
207 and the Entactinaria: evidence from the middle Cambrian Inca Formation, Georgina Basin, Australia, and Lower
208 Ordovician Cow Head Group, Newfoundland. *Journal of Paleontology*, 1-24 doi:
209 <https://doi.org/10.1017/jpa.2026.10215>
- 210 Sheng J, Aitchison JC, Kachovich S, Arhatari BD, Stevenson AW, Ye Y, Liu S (2026) Unlocking a hidden fossil archive:
211 synchrotron micro-computed tomography illuminates ‘ghost’ radiolarians linked to Late Ordovician oceanic anoxic
212 events. *Royal Society Open Science* 13: 252091. <https://doi.org/10.1098/rsos.252091>
- 213 Won M-Z, Below R (1999) Cambrian radiolarians from the Georgina Basin, Queensland, Australia. *Micropaleontology* 45:
214 325-363.
- 215 Won M-Z, Iams WJ, Reed KM (2005) Earliest Ordovician (Early to Middle Tremadocian) Radiolarian faunas of the Cow
216 Head Group, Western Newfoundland. *Journal of Paleontology* 79: 433-459.
- 217 Won M-Z, Iams WJ (2002) Late Cambrian radiolarian faunas and biostratigraphy of the Cow Head Group, western
218 Newfoundland. *Journal of Paleontology* 76: 1-33.
- 219
220
221
222
223
224
225
226
227
228
229
230

231

232

233 **Captions**

234



235

236 **Figure 1.** Illustration of the scanned radiolarian specimen. Scale = 250 μm

237

238

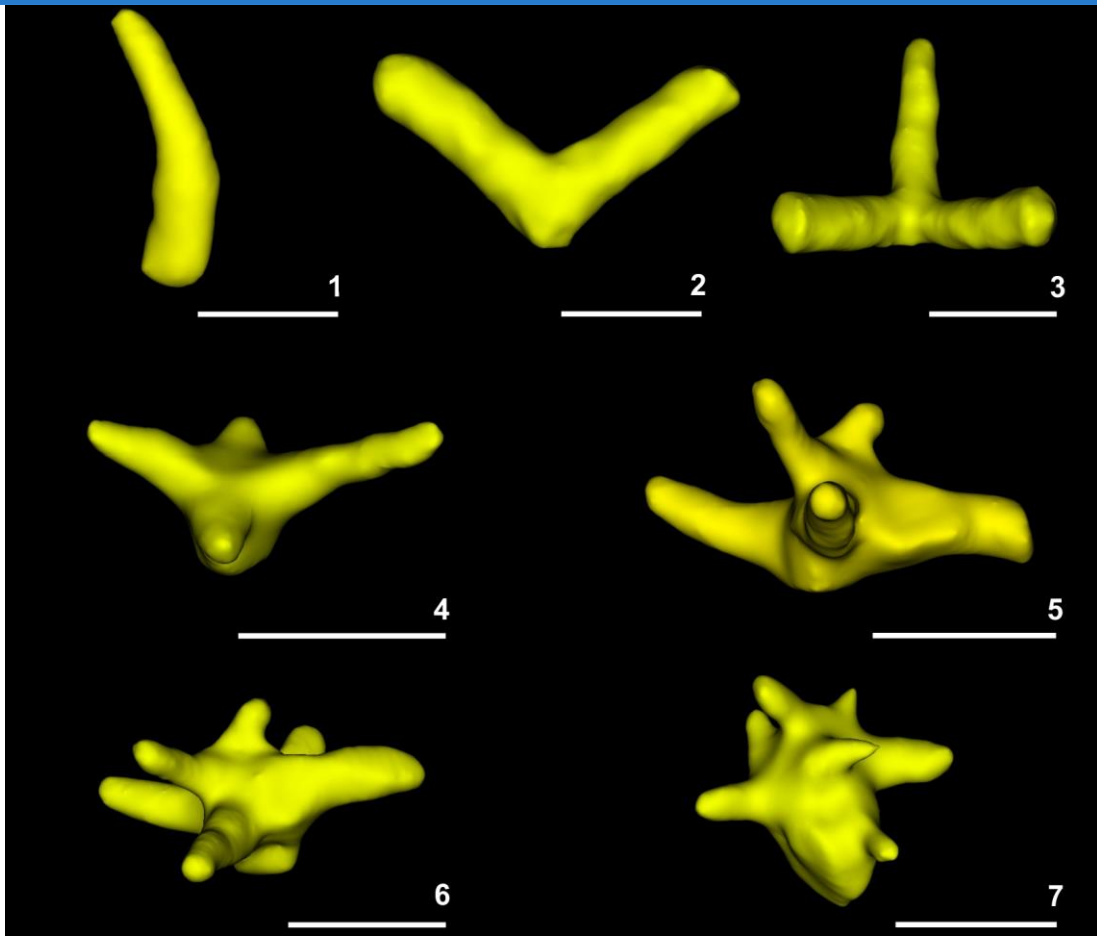
239

240

241

242

243



244

245 **Figure 2.** Different types of branches and number of rays per branch recognised in this study. 1) Single
246 ray; 2) bifurcating; 3) trifurcating; 4) quadrifurcating; 5) pentafurcating; 6) hexafurcating; 7)
247 heptafurcating.

248

249

250

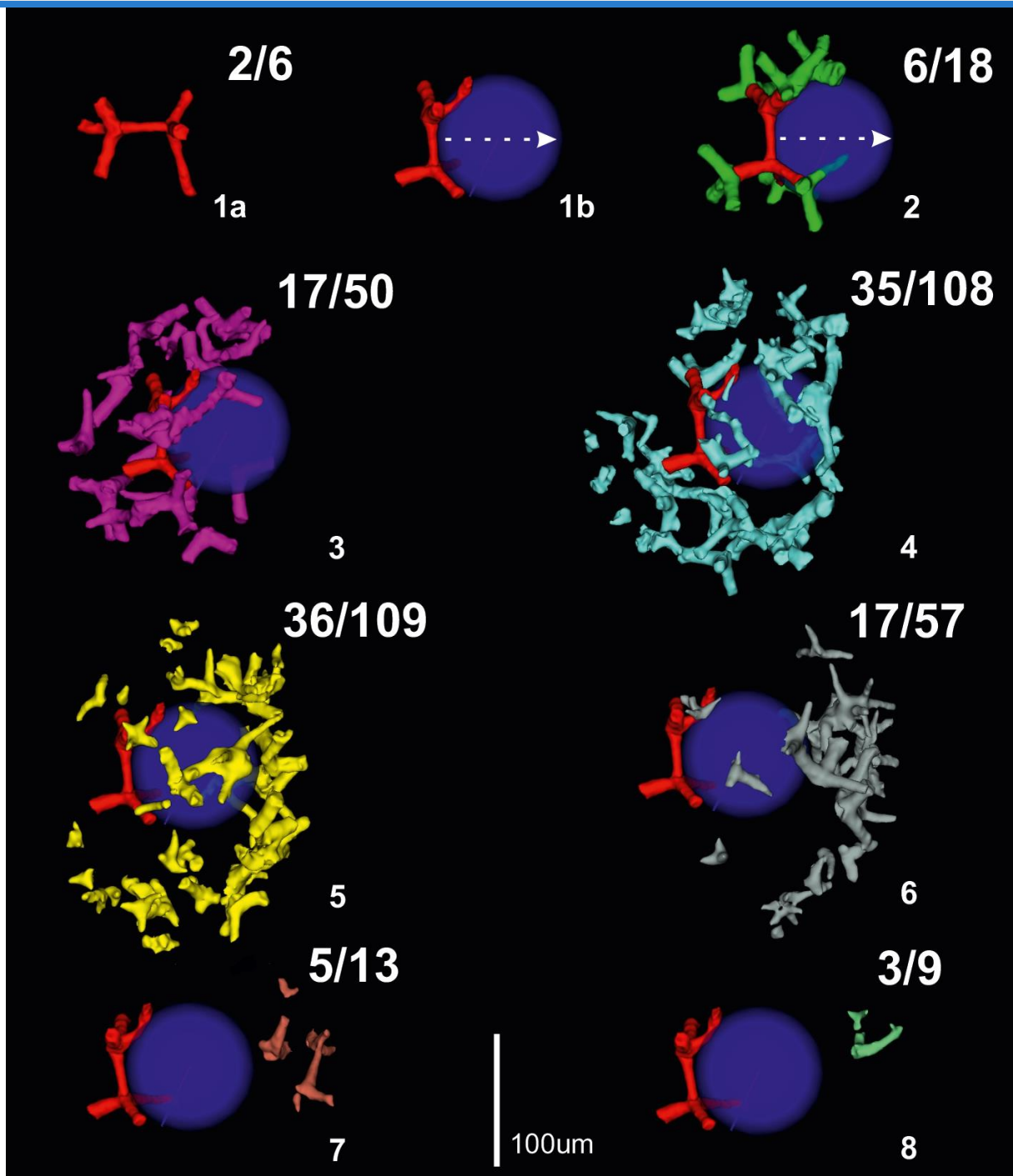
251

252

253

254

255



256

257 **Figure 3.** Successive growth stages of branches of the skeleton of *Protoentactinia gracilispinosa*.

258 Numbers indicate new branches/rays.

259

260

Grow th stage	Sing le ray	Bifurca- ting	Trifurca- ting	Quadrifur- cating	Penta- furcating	Hexafurca- ting	Hepta- furcating	Total of new branch es	To- tal of new rays
Stage 1	0	0	2	0	0	0	0	2	6
Stage 2	0	0	6	0	0	0	0	6	18
Stage 3	0	2	14	1	0	0	0	17	50
Stage 4	1	5	23	4	0	2	0	35	108
Stage 5	2	7	18	6	3	0	0	36	109
Stage 6	1	1	10	3	1	0	1	17	57
Stage 7	0	2	3	0	0	0	0	5	13
Stage 8	0	1	1	1	0	0	0	3	9

261

262 **Table 1** : Number of new rays and type of branches produced at each growth stage of the skeleton of

263 *Protoentactinia gracilispinosa*.